

Elixir: A system to enhance data quality for multiple analytics on a video stream

Sibendu Paul
Purdue University
West Lafayette, USA

Kunal Rao
NEC Laboratories America, Inc.
New Jersey, USA

Giuseppe Coviello
NEC Laboratories America, Inc.
New Jersey, USA

Murugan Sankaradas
NEC Laboratories America, Inc.
New Jersey, USA

Oliver Po
NEC Laboratories America, Inc.
San Jose, USA

Y. Charlie Hu
Purdue University
West Lafayette, USA

Srimat Chakradhar
NEC Laboratories America, Inc.
New Jersey, USA

ABSTRACT

IoT sensors, especially video cameras, are ubiquitously deployed around the world to perform a variety of computer vision tasks in several verticals including retail, healthcare, safety and security, transportation, manufacturing, etc. To amortize their high deployment effort and cost, it is desirable to perform multiple video analytics tasks, which we refer to as Analytical Units (AUs), off the video feed coming out of every camera. As AUs typically use deep learning-based AI/ML models, their performance depend on the quality of the input video, and recent work has shown that dynamically adjusting the camera setting exposed by popular network cameras can help improve the quality of the video feed and hence the AU accuracy, in a single AU setting.

In this paper, we first show that in a *multi-AU setting*, changing the camera setting has disproportionate impact on different AUs performance. In particular, the optimal setting for one AU may severely degrade the performance for another AU, and further the impact on different AUs varies as the environmental condition changes.

We then present Elixir, a system to enhance the video stream quality for *multiple* analytics on a video stream. Elixir leverages Multi-Objective Reinforcement Learning (MORL), where the RL agent caters to the objectives from different AUs and adjusts the camera setting to simultaneously enhance the performance of all AUs. To define the multiple objectives in MORL, we develop new AU-specific quality estimator values for each individual AU. We evaluate Elixir through real-world experiments on a testbed with three cameras deployed next to each other (overlooking a large enterprise parking lot) running Elixir and two baseline approaches, respectively. Elixir correctly detects 7.1% (22,068) and 5.0% (15,731) more cars, 94% (551) and 72% (478) more faces, and 670.4% (4975) and 158.6% (3507) more persons than the default-setting and time-sharing approaches, respectively. It also detects 115 license plates, far more than the time-sharing approach (7) and the default setting (0).

1 INTRODUCTION

Due to the spurring demand for automation and the impetus to make everything "smart", IoT sensors are increasingly being deployed and there has been rapid technological advancement to

utilize raw sensor data and generate actionable insights from them. The global smart sensor market size is expected to grow from \$37 billion in 2020 to \$90 billion by 2027 at a CAGR of 14% [1]. Among these IoT sensors, video cameras are very popular, since they act as our "eyes" to the world and many important video analytics tasks, which we refer to as Analytical Units (AUs), are performed on the raw visual data feed from video cameras.

Deploying cameras requires enormous effort and investment, and thus there is often expectation to get the most out of the deployed cameras, by running multiple AUs on each video stream to generate multiple, different insights. For example, as shown in Figure 1, from a single video camera feed, AUs like person detection, motion/pose estimation, face detection, face recognition (to identify VIP/person of interest), age prediction, gender classification, license plate detection, license plate recognition, accident prediction, etc. can be performed. For a camera deployed in a store, further analytics such as the number of unique visitors, flow of people inside the store, congregation of people, time spent by visitors in different sections, etc. can be performed. All such information is very useful for store safety, store analytics, and improvement of conversion rate. As another example, for video feed off a camera deployed at a road intersection, multiple AUs like vehicle detection, license plate detection and recognition, pedestrian detection, vehicle speed detection, red light crossing detection, accident prediction, etc. can be performed. There are many more scenarios where a camera is deployed in an enterprise building, stadium, bank, or factory, etc., and multiple different AUs are run at the same time to generate insights. Sometimes high level AUs are dependent on multiple low level AUs to generate insights and in such scenarios we need joint optimization for multiple AUs. For example, for an accident prediction AU, detection of pedestrians, cars, their speed of movement, etc. all have to work well and these tasks serve as building blocks for the accident prediction AU.

AUs typically use deep-learning based AI/ML models, which act as our "brains" to process the visual data seen through the "eyes" of video cameras. These models are developed by building deep neural networks (DNNs) and training these networks with thousands of images. This process leads to some "trained" models, that are capable of performing specific computer vision tasks, e.g.,

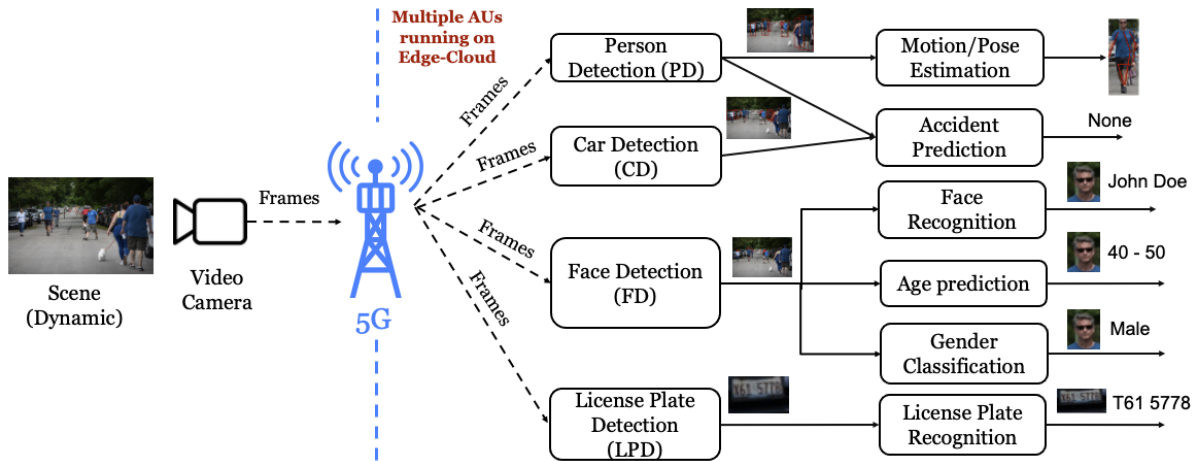


Figure 1: Multiple AUs running on a single video stream.

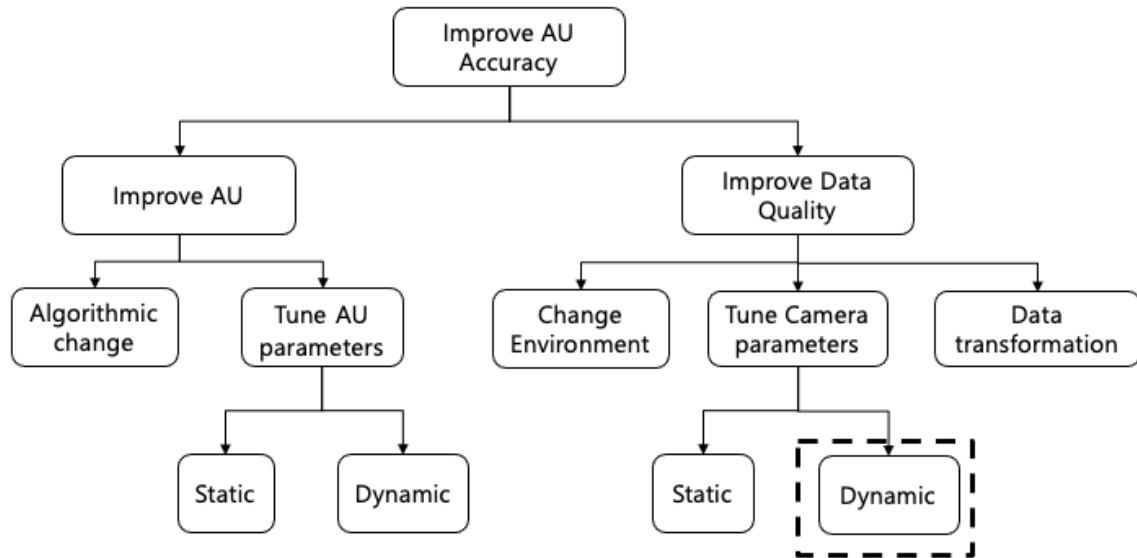


Figure 2: A taxonomy of possible techniques to improve AU accuracy in video analytics.

object detection. As such, it is very important for these models to be highly accurate for the generated insights to be useful.

There are two general approaches towards improving the accuracy of an AU in a video analytics system, as shown Figure 2: improving the AU design and improving the quality of video stream. In the first approach, one can improve the accuracy of the AU by making algorithmic changes in the underlying DNN model. This, however, is a very expensive and slow solution, because it is not practical to keep training the model with new algorithms and new datasets on costly GPU resources. Another way to improve the AU is by tuning AU parameters, which can be done either at the start, i.e., statically, or during operation, i.e., dynamically. One example of AU parameters is the minimum number of pixels between eyes, which is used for “face detection” AU. This configurable parameter

can be tuned to determine faces in the scene. However, depending on the environmental conditions around the camera (lighting conditions), the content in the scene (number of faces, speed of movement of people), the settings of the camera (brightness, contrast, color, sharpness, exposure, shutter speed), etc., the quality of image obtained from the camera can vary. As a result, adjusting the configuration value for “minimum pixels between the eyes” after the image acquisition from the camera may not be able to improve the AU accuracy if the video frame itself is not of good quality.

The second general approach to improving AU accuracy is to improve the quality of data that is fed to the AU. Intuitively, if the AU receives “good” quality input data, e.g., similar to what it has seen during “training”, the chances of the AU producing accurate results is high. There are three different ways in which we can improve the quality of input data to the AU, namely, (1) improving

the environment around the camera, e.g., by adding additional light, such that the camera is able to get a better capture of the scene, (2) applying data transformation on individual frames of the video feed captured by the camera, and (3) tuning camera parameters in order to help the camera capture good quality video. Changing the environment is not practical in different scenarios and applying data transformation is typically too late because the camera has already captured the scene. Therefore, in this paper, we focus on tuning camera parameters. A similar approach has been studied in [24], which, however, has only considered single-AU scenarios. Unlike [24], in this paper, we only consider *multiple* AUs at the same time and study how to dynamically tune the camera setting for multiple AUs.

Tuning camera parameters for a single AU itself is already challenging because the optimal camera parameters for an AU keep changing as the environmental condition and the video content change over time, and the camera comes with thousands of possible camera settings even for a handful of parameters, as shown in [24]. When there are multiple different AUs running at the same time on a single camera feed, the problem of dynamic camera settings adjustment becomes even more challenging. The key reason is that the optimal camera settings for one AU may degrade performance for another AU and vice versa, as shown in our experiments. In particular, each AU has some optimal camera setting but when multiple AUs all work off the same camera feed, which can assume only one physical camera setting at any given point in time, the camera setting that is “good” for all AUs at the same time is extremely difficult to identify. In this paper, we tackle this challenging problem and present Elixir, a system that dynamically finds the optimal camera setting that enhances input video quality such that the performance of multiple different AUs, which are running off the camera feed, are improved simultaneously.

Elixir is an online system, meaning it dynamically tunes camera settings while the AUs are in operation, i.e., in reaction to environmental condition and scene change. Making such dynamic adjustment faces a fundamental design challenge – how to estimate the quality of the current camera setting, i.e., the accuracy of the AUs, as it is not possible to measure AU accuracy online using traditional methods, which require ground truth information. To address this challenge, we develop and use new AU-specific quality estimators, which analyze a frame and estimate the quality of the frame for the specific AU accuracy. The higher the quality, the more likely that the AU will have high accuracy on the frame. With the set of AU-specific quality estimators, one for each AU, the goal of Elixir is to dynamically identify the camera settings that will lead to high values on the AU-specific quality estimates. To do so, Elixir leverages Multi-Objective Reinforcement Learning (MORL) in which the multiple objectives correspond to the different AU-specific quality estimates (one per AU) and the goal for the RL agent is to maximize the combined value of an aggregate objective function that incorporates quality estimate values from all the AUs running on the single video stream.

In summary, the key contributions of this paper are:

- We show that when *multiple* AUs run on a single video camera feed, the optimal camera setting for one AU degrades accuracy of another AU, i.e., they conflict with each other.
- We present Elixir, a system that leverages Multi-Objective Reinforcement Learning (MORL) to enhance the quality of input camera feed to AUs by dynamically finding the optimal camera setting by training the RL agent to maximize the aggregate quality estimate for all AUs.
- We develop new AU-specific quality estimators for multiple different AUs, including face detection, person detection, car detection and license plate detection, and show that these can be used as proxies for estimating AU accuracy in the absence of ground truth, which is not practical to obtain during real-time operation of the AUs.
- We perform real-world experiments with three cameras running multiple AUs on each cameras at the same time, wherein the first camera uses the default camera settings, the second one uses time-sharing technique to favor one particular AU during its time share, and the third uses Elixir. Our results show that when compared to using the default camera settings and the time-sharing approach, Elixir correctly detects 7.1% (22,068) and 5.0% (15,731) more cars, 94% (551) and 72% (478) more faces, and 670.4% (4975) and 158.6% (3507) more persons, respectively. It also detects 115 license plates, far more than the time-sharing approach (7) and the default setting (0).

The rest of the paper is organized as follows. Section 2 discusses related work. Section 3 motivates the need for Elixir. Next, Section 4 discusses the various challenges encountered in designing Elixir and our approach to overcome those challenges. Elixir’s overall system design is shown in Section 5 and results are presented in Section 6. Finally, we discuss further possible improvements using digital transformation in Section 7 and conclude in Section 8.

2 RELATED WORK

Applying multiple AUs on a single camera video stream is explored in MultiSense [26] and Panoptes [10], but they consider AUs which require different views from the camera. To support these AUs at the same time, they propose to use PTZ cameras, which can be remotely controlled to change the view of the camera as per the need of the AU. They multiplex multiple AUs through time-sharing approach and via view virtualization. This way, multiple AUs can run on a single video stream. However, in this paper, we consider multiple AUs that run together on the *same* view of the camera and there is no need to control and change the view of the camera. In such a setup, we show that each AU has an optimal camera setting to achieve highest accuracy for the AU, but these optimal camera settings conflict with each other i.e. optimal camera setting for one AU degrades accuracy for another AU. Such conflict across multiple AUs is not considered in MultiSense [26] and Panoptes [10].

Along with multiple AUs running off of a single camera stream, there are also several works which focus on single AU running off of multiple cameras. Most recent work, VeTrac [29] employs widely deployed traffic cameras as a sensing network for vehicle tracking at large scale. [5, 25] propose to automatically capture high quality surveillance video through distributing targets to different co-located cameras. Yao *et al.* [30] adaptively assign several PTZ cameras based on the moving objects in a multi-camera, multi-target surveillance system. In this paper, we do not consider such

multi-camera scenario, but focus on single camera, multiple AUs running off of this single camera.

Changes in environmental conditions have direct impact on the accuracy of the AU as shown in [24]. To alleviate the degradation in AU accuracy due to environmental changes, Jang *et al.* [11] propose IoT camera virtualization and support multiple AUs, each using different AI/ML model, which is appropriate for the specific environment. These multiple AUs, however, are to generate similar insight and only one of them runs at any given point in time. In contrast, in this paper, we consider multiple AUs, each generating different insights and they all run simultaneously at the same time.

To improve accuracy for single AU, few recent works, *e.g.*, AMS [15], Focus [8], Ekya [23], and NoScope [14], studied dynamic AU model parameters tuning based on captured video content. Although it is a plausible approach to extend this method for multiple AUs, but the periodic model training on expensive GPU resources and slow reaction to dynamic changes, makes this approach non-feasible for practical deployment.

Several works *e.g.*, Chameleon [12], Videostorm [32], and AW-Stream [31] adapt camera settings like frame resolution and frame per second (fps) while processing single AU. Their goal is to make it efficient to run video analytics tasks, while the goal for Elixir is to improve AU accuracy for multiple AUs running off of a single video stream. Thus, although we could extend this work for multiple AUs, since the goal is different, we chose not to go with these camera settings, which make sense to change from efficiency point of view but not from improving AU accuracy point of view.

The most recent work, CamTuner [24] dynamically tunes the four camera settings considered in this paper, in response to changes in environmental conditions in order to improve the accuracy of a video analytics pipeline. However, CamTuner focuses on improving accuracy of a single AU running on a camera stream. In practice, multiple AUs typically run off of a single camera stream (*e.g.*, FD, PD, CD, LPD, *etc.* as shown in Figure 1), and this multiple AUs scenario is not addressed by CamTuner. Similar to CamTuner, in this paper, we focus on the four camera settings *i.e.* brightness, contrast, color and sharpness, but the changes done to these settings in CamTuner is with respect to a single AU. In contrast, Elixir dynamically changes these settings in order to cater to multiple AUs. In this paper, we use AU-specific quality estimator, which was introduced in CamTuner, but we develop new one's for PD, FD, CD and LPD AUs. In CamTuner, since there is only a single AU, there is no question of conflict across AUs, while in Elixir, camera settings for one AU conflicts with another AU. For instance, an increase in brightness of the entire capture might be beneficial for coarse-grained person or car detection but it can hurt fine-grained face detection and facial recognition, as the face area get overexposed. Thus, challenges solved by Elixir are different from the one's solved by CamTuner. To the best of our knowledge, this is the first work that addresses the challenge of improving accuracy for multiple AUs running off of a single camera stream by dynamically tuning camera settings, which enhances data quality such that accuracy of multiple AUs is improved simultaneously.

3 MOTIVATION

In this section, we first show that different AUs benefit from different camera settings, *i.e.*, the optimal camera setting for different



Figure 3: Scene for multiple AU experiments

Table 1: Optimal camera settings for different AUs.

AU	Optimal Camera Setting [brightness, contrast]	Additional detections (over default setting)
FD	[30,80]	89
PD	[40,80]	52
CD	[65,30]	2
LPD	[80,65]	14

AUs differ at any given point in time. Then, we systematically study the impact of optimal camera settings for different AUs and show optimal camera settings conflict, *i.e.*, the optimal camera setting for one AU degrades performance of another AU.

Finally, we show that there exists some camera setting that works well for multiple AUs at the same time, which motivates us to study automatically finding such a setting while the system is in operation.

Since any video camera can have only one camera setting at any given point in time, it is impossible to design experiments to study the effect of different camera settings on different AUs at the same time, for the same exact input scene. The closest alternative is to use multiple cameras, with different setting for individual AUs. However, there are thousands of possible camera settings, and it is not practical to have as many cameras to cover all settings for the same input scene. As a work around, we chose two alternatives: (1) Fix a static input scene in a controlled setting, point the video camera to this scene and run multiple AUs with different camera setting on this single camera. This way, we can obtain accuracy for the AUs with different camera setting for the same input scene (in a controlled environment). (2) Use two side-by-side cameras, one with the default camera setting and another with "modified" camera setting, and then recreate and repeat the exact same sequence of steps in the scene, thereby providing similar input video content/scene for different "modified" camera settings, and measure the resulting AU accuracy. In all our experiments, we modify four popular camera settings, *i.e.*, *brightness*, *contrast*, *color-saturation* (also known as *colorfulness*), and *sharpness*, which are commonly found in almost all video cameras. All other camera settings are kept at manufacturer-provided default values.

3.1 Optimal camera setting varies across AUs

3.1.1 Different AUs have optimal camera settings. In [24], it is shown that optimal camera settings for a *single* AU is not the same all the time, *i.e.*, it changes as the environmental condition and video content change over time. In this section, we show that the optimal camera settings is not the same for *different* AUs at any

given point in time. Since we do not have any public datasets that have identical videos captured with different camera settings, we created our own video dataset. To collect a video in the dataset, we place two side-by-side cameras at a parking lot and have two participants repeat the following sequence of steps: drive the car towards the camera, show their face, drive past the camera, park the car, walk towards the camera and walk past the camera. The two side-by-side cameras used were Axis Q3505 MK II Network camera, each capturing frames at 10 FPS and the scene observed by the cameras is shown in Figure 3. The sequence of steps followed by the two participants allows us to perform multiple analytics, namely, car detection (CD), person detection (PD), face detection (FD) and license plate detection (LPD) on a single video stream and obtain results for different “modified” camera settings. In total, we repeated the sequence of steps for 26 different camera settings and observed the resulting AUs accuracy on each of the “modified” camera setting.

Table 1 shows that for the four AUs that run simultaneously on the video with the same “modified” camera setting, each AU has a different camera setting that gives the highest accuracy for the AU. For example, FD has highest accuracy with brightness set to 30 and contrast set to 80, while CD has highest accuracy with brightness set to 65 and contrast set to 30. All our results are normalized to the detections obtained with the default camera setting, and the “modified” camera setting which shows the highest number of additional detections ¹ over the default setting (shown in the right most column in Table 1) is considered the optimal camera setting for the specific AU. From Table 1, we can clearly see that all four AUs have different optimal camera setting, i.e., the camera setting that gives the highest accuracy for the AU. Thus, *optimal camera setting varies across AUs*.

3.1.2 Optimal camera settings conflict. In Section 3.1.1, we saw that different AUs have different optimal camera setting at any given point in time. Assume that there are two AUs, say AU_1 and AU_2 with optimal camera settings as S_1 and S_2 , respectively. Now, since the camera can have only one setting at any given point in time, what happens to AU_2 's accuracy if the camera setting is S_1 and vice versa, i.e., what happens to AU_1 's accuracy if the camera setting is S_2 ? To perform such a study, we set up two controlled experiments and show below that there exists a conflict between the AUs, i.e., the optimal camera setting for one AU degrades performance of another AU.

For the first controlled experiment, we print 12 different person cutouts obtained from the COCO dataset [18] and place them in front of a real camera. Next, we use two sources of light. One is always turned ON and the other is turned ON to simulate DAY condition and the turned OFF to simulate NIGHT condition. By using two sources of light, we can change the environmental conditions around the camera by just turning one source of light ON or OFF. In addition, we set up a controlled experiment with 3D models of people and cars being observed by the AXIS Q3515 camera and then show the conflict between PD, FD and car detection (CD) on this second setup.

Table 2 shows the conflict when we apply optimal camera settings of PD to FD and vice versa for DAY and NIGHT conditions.

¹We manually verified that these additional detections were all true positive detections

Table 2: Optimal camera settings conflict (2D printouts).

AU	Optimal camera setting [brightness, contrast color, sharpness]	FD accuracy mAP (%)	PD accuracy mAP (%)
PD	[40,90,60,100]	82.58	99.36
FD	[60,40,90,90]	100.0	83.33

(a) DAY

AU	Optimal camera setting [brightness, contrast color, sharpness]	FD accuracy mAP (%)	PD accuracy mAP (%)
PD	[80,90,70,100]	38.89	83.33
FD	[80,90,60,80]	50.0	75.0

(b) NIGHT



Figure 4: Controlled experiment with 3D models.

Table 3: Optimal camera settings conflict (3D models).

Optimal camera setting [brightness,contrast, color,sharpness]	FD accuracy mAP (%)	PD accuracy mAP (%)	CD accuracy mAP (%)
FD [60,30,40,80]	52.1	78.7	54.5
PD [80,60,50,40]	37.3	100.0	66.7
CD [70,50,60,60]	41.9	85.8	96.9

For DAY condition, the optimal camera setting for PD (brightness: 40, contrast: 90, color: 60, sharpness: 100) gives 99.36 % accuracy for PD but the same camera setting gives only 82.58 % accuracy for FD, which with another camera setting, i.e., brightness: 60, contrast: 40, color: 90, sharpness: 90, achieves 100 % accuracy. Conversely, when we apply optimal camera setting for FD to PD, then the accuracy of PD drops from 99.36 % to 83.33 %. Similar observation holds for NIGHT condition as well, as shown in Table 2b. Here, the optimal setting for FD achieves 50 % accuracy, but the accuracy drops to 38.89 % accuracy if the optimal setting for PD is applied to FD. Also, the optimal setting for PD achieves 83.33 % accuracy but the accuracy drops to 75 % if the optimal setting of FD is applied to PD.

For the second controlled experiment, we set up 3D models of people and cars as shown in Figure 4. Here, we modify the values of four camera parameters, i.e., brightness, contrast, color and sharpness, each from 0 to 100 in steps of 10, and capture the image from the camera for each of the “modified” setting. In total,

Table 4: Common good camera settings across AUs.

Camera Setting	FD accuracy mAP (%)	PD accuracy mAP (%)
Default	82.58	90.9
PD-optimal	82.58	99.36
FD-optimal	100.0	83.33
<i>Common-optimal</i>	100.0	91.7

(a) DAY

Camera Setting	FD accuracy mAP (%)	PD accuracy mAP (%)
<i>Default</i>	38.89	58.3
PD-optimal	38.89	83.38
FD-optimal	50.0	75.0
<i>Common-optimal</i>	48.8	83.3

(b) NIGHT

we obtain $\approx 14.6K$ (11^4) different images corresponding to different camera settings and run three different AUs, i.e., PD, FD and CD on each of these images. Table 3 shows the conflict observed for these three AUs. The optimal setting for FD achieves 52.1 % accuracy, but the accuracy drops to 37.3 % when the optimal setting of PD is applied to FD, and to 41.9 % when the optimal setting for CD is applied to FD. Similarly, PD achieves 100 % accuracy under its own optimal setting, but only 78.7 % accuracy when the optimal setting for FD is applied, and 85.8 % when the optimal setting of CD is applied. As with FD and PD, conflict is also observed for CD. The CD accuracy is 96.9 % under its own optimal setting, but drops to 66.7 % and 54.5 % when the optimal settings for PD and FD are applied, respectively. *Thus, the optimal camera settings of AUs conflict with each other when multiple AUs are run simultaneously.*

3.2 Common-optimal camera settings exists

In Section 3.1.1 we saw that different AUs have different optimal camera setting at any given point in time, and in Section 3.1.2 we saw that optimal camera setting across AUs conflict with each other, i.e., the optimal setting for one AU degrades performance of another AU. In this section, we show that there exists a common-optimal camera setting that works well across multiple AUs. This motivates us to automatically find this common-optimal camera setting during online operation of the video analytics system.

We use the same setup as discussed in Section 3.1.2 with two sources of light. Table 4 shows the accuracy for FD and PD for different camera settings, i.e., the default camera setting, optimal camera setting for PD (PD-optimal), optimal camera setting for FD (FD-optimal), and common-optimal camera setting (*Common-optimal*) for DAY and NIGHT conditions. In this experiment, we define the common-optimal setting as the one that gives the highest cumulative accuracy of the two AUs (PD and FD). Section 5.1 discusses alternative definitions of common-optimal setting according to how the accuracy estimates of multiple AUs are aggregated.

Table 4a shows that with common-optimal camera setting, we are able to restore the drop in FD accuracy from 100 % to 82.58 %, back to 100 %. Also, due to the conflict, PD accuracy dropped from 99.36 % to 83.33 %, but with the common-optimal camera setting, we

are able to bump it up to 91.7 %. We see similar improvement in accuracy with common-optimal camera settings for NIGHT condition as well, as shown in Table 4b. *Thus, there exists a common-optimal camera setting, which works well across multiple AUs.*

4 CHALLENGES AND APPROACHES

In this section, we describe the key challenges that we face in order to alleviate the ill-effects of one AU camera setting on another AU, and improve the accuracy of multiple AUs (running on a single camera stream) simultaneously.

Challenge 1: How to define the common-optimal camera setting? As discussed in Section 3, the camera setting has a direct impact on the accuracy of AUs and when there are multiple AUs running on a single video stream, depending on the camera setting, some AUs may perform better while others perform worse. To improve accuracy of multiple AUs simultaneously on a single video stream, we need to choose a camera setting that optimizes the aggregate accuracy for all AUs, a.k.a. the common-optimal camera setting. Depending on the AU, the acceptable accuracy may vary and for certain AUs, accuracy improvement over a certain threshold may not be very significant. Therefore, it is not so straightforward to define the common-optimal camera setting, which gives optimal performance across multiple AUs.

Approach. Since the meaning of the change in accuracy numbers varies across AUs and there is no generic method to determine "optimal" accuracy for any given AU, we choose to define an objective function that aggregates the accuracy for multiple AUs into a single metric. The objective function allows for different aggregation strategies, which are defined by domain experts, and we design Elixir to choose the camera setting that optimizes the aggregate objective function, which works the best across multiple AUs.

Challenge 2: How to achieve common-optimal camera settings for a particular scene for multiple AUs? Defining the common-optimal camera setting is one thing, but achieving the common-optimal camera setting is whole another thing. As the scene in front of the camera changes (due to environmental changes, lighting condition changes or change in flow of people/objects, etc.), the accuracy of AUs also changes, and thus the common-optimal camera setting for the particular scene also changes. This change of scene is inevitable and continuous, and it is quite challenging to adapt to such changes and achieve the common-optimal camera setting for a particular scene for multiple AUs in real-time.

Approach. One way to find the common-optimal camera setting for a particular scene for multiple AUs is to train a model that knows the various scenes and for the specific combination of the AUs, so that it can provide the common-optimal camera setting for any given scene. However, training such a model is almost impractical, since we do not know a priori the various conditions that would be observed by the cameras at various locations. Therefore, our approach is to use online learning, where the common-optimal camera setting for the specific AUs is learned in an online fashion, after the camera is deployed.

Challenge 3: No Ground truth during online operations. Implicit in the definition of the common-optimal camera setting is the accuracy of individual AUs. To determine the accuracy of AUs, it is essential to know the ground truth, so that one can compare the

results with the ground truth and determine the accuracy. However, knowing such ground truth during online operations is not possible, since there is no human in the loop to annotate the frames in real-time. In such a scenario, how can we determine the common-optimal camera setting for multiple AUs running on a single video stream?

Approach. Since we do not have actual ground truth in real-time and we cannot determine the exact accuracy of AUs, we choose to *estimate* the accuracy of the AUs using proxy, similarly as in [24]. Since each AU has a different method of measuring accuracy, our proxy is also different for each AU and we keep it light-weight, so that we can *estimate* the accuracy in real time. By using light-weight, AU-specific quality estimator, we compensate for the lack of availability of ground truth in real-time.

Challenge 4: Extremely slow online learning. Online learning helps us to achieve common-optimal camera settings for a particular scene for multiple AUs. However, the learning is extremely time consuming. This is because, it takes a very long time to undergo various conditions and as part of online learning, every change in camera settings takes a long time (~ 200 ms). This limits the speed of online learning to the point that it can become ineffective.

Approach. We pre-learn (offline) the values of various AU-specific estimates for different AUs depending on the measured values of brightness, contrast, color and sharpness for the images and corresponding camera setting values. This helps in accelerating the learning process when the camera is deployed in operation, because the online learning agent is already bootstrapped with some pre-computed values which allows it to start exploration and exploitation immediately.

5 DESIGN

In this section, we discuss Elixir’s overall system design and its two key components, the Multi-Objective Reinforcement Learning (MORL) agent and AU-specific Quality Estimators, which aid in dynamically finding the common-optimal camera settings that enhances the input video quality, such that the accuracies of multiple AUs running on a single video stream are improved simultaneously.

Figure 5 shows the overall system design for Elixir. As the scene in the field of view of the camera changes dynamically, the video camera captures the input scene and depending on the camera settings, emits frames, which are then transmitted over 5G network to different AUs for further processing. In parallel, frames are also transmitted to the *AU-specific quality estimators* and the *MORL agent*. AU-specific quality estimators provide estimates for the quality of the frames that correlates with the AU-specific accuracy; the higher the quality, the better chances the AU will give high accuracy on the frame. The MORL agent obtains the quality estimates from individual AU-specific quality estimators, combines them into an aggregate single value for the frame, and learns to tune the camera settings to a common-optimal setting that works well for multiple AUs simultaneously. Next, we discuss the two key components, MORL and AU-specific quality estimators, in detail.

5.1 Multi-Objective Reinforcement Learning

Reinforcement Learning (RL) is a popular technique for online learning where the agent observes the environment (*state*) that it is

in, performs an *action* among the allowed set of actions and learns to maximize a *reward* function, which is set up in order to achieve the desired goal. In [24], only a *single* AU was considered, and therefore, a single-objective, traditional RL technique could be used to tune the camera settings to improve accuracy of a single AU. However, for Elixir, there are *multiple* AUs running simultaneously and the goal is to improve the accuracy for all of them simultaneously. Hence, we use a Multi-objective Reinforcement Learning (MORL) [7, 19] technique with multiple objectives (one for each AU) to find the common-optimal camera setting that enhances the data quality such that the accuracies of multiple AUs are improved simultaneously.

Figure 6 shows the difference between traditional RL and MORL. In traditional RL, the agent receives only a single reward, whereas in MORL the agent receives multiple rewards, one corresponding to each objective. The goal of the MORL agent is to improve all these individual rewards. In our case, we have multiple AUs running off of a single video stream and the goal is to improve accuracy for each of these AUs. This accuracy for each AU is determined by the reward that the agent obtains for each AU. Now, if the action taken by the agent improves the accuracy of the AU, then the reward is positive, otherwise it is negative. Elixir uses AU-specific quality estimators (discussed in Section 5.2) as reward function for each AU.

Next, we define the *State*, *Action* and the *Reward* used by the MORL agent in Elixir.

State: State is a tuple of two vectors, $s = \langle P_t, M_t \rangle$, where P_t consists of the values of brightness, contrast, color and sharpness in the camera settings at time t , and M_t consists of the measured values of brightness, contrast, color and sharpness of the captured frame at time t .

Action: The set of actions for the MORL agent are (a) to increase or to decrease camera setting value for brightness, contrast, color or sharpness (only one among the four) (b) no change to any camera setting values. Thus, in total, there are 9 actions – increasing or decreasing one of the four camera settings (8 actions) and no change (the 9th action).

Reward: Value of an aggregate function that combines the values of AU-specific quality estimators for all the AUs running off of the single video camera stream.

Several methods can be used by the MORL agent in using the individual reward functions and “learning” to take appropriate actions. The learning process by the agent leads to a “policy”, which guides the agent in taking actions leading to common-optimal camera settings. Now, there can be “single-policy” or “multiple-policies” algorithms that can be used in MORL [7, 19]. As pointed out in [7], “single-policy” algorithms are more appropriate when the aggregation function, a.k.a. utility function or scalarization function, is known apriori and does not change over time, whereas “multi-policy” algorithms are more appropriate when the aggregation function is not known or changes over time. In Elixir, we define our own aggregation function which is not changed over time. Thus, “single-policy” algorithm is preferable by the MORL agent in Elixir. In this method, the MORL agent addresses the multi-objective problem by using the aggregation function to reduce the multi-objective problem into a single-objective problem, where the individual reward values are aggregated into a single reward value.

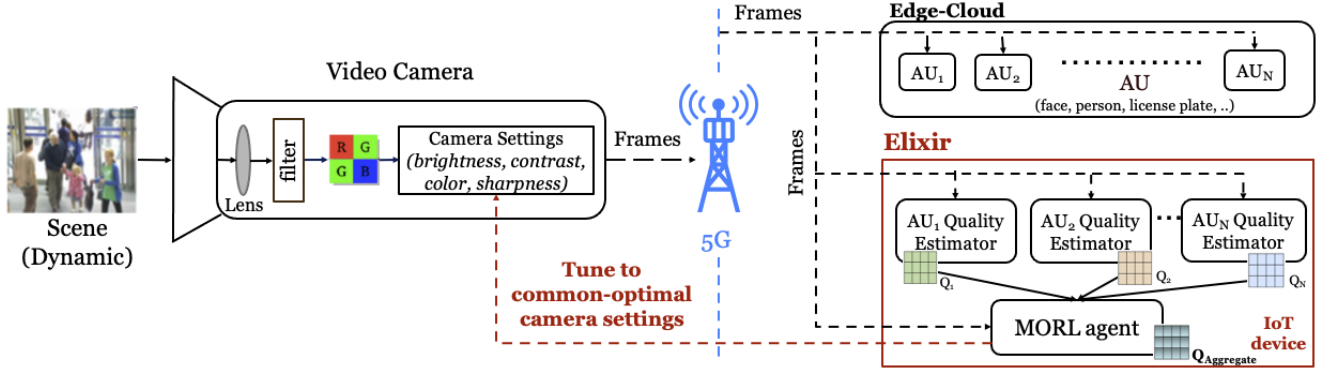


Figure 5: Elixir system design.

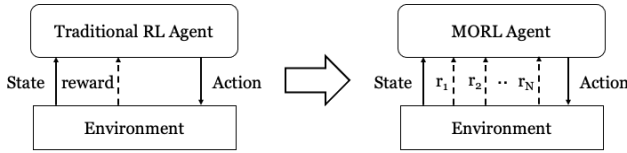


Figure 6: Traditional RL vs MORL architecture

Algorithm 1: Single-policy approach to MORL

Input: N = Number of AUs/objectives
Input: K = Number of episodes

- 1 Initialize State s
- 2 Initialize Q table for each AU and $Q_{aggregate}$ ($N+1$ Q-tables)
 // During exploration upto episode K
- 3 **while** Still-Processing() **do**
- 4 $a \leftarrow$ Choose-Action($Q_{aggregate}, s$)
- 5 Perform-Action(a)
- 6 $s' \leftarrow$ Observe-Environment()
- 7 **for** $AU_i = 1, 2, \dots, N$ **do**
- 8 // AU-specific quality estimation
- 8 $r_i \leftarrow$ Compute-Reward()
- 8 // Bellman optimality equation
- 9 $Q_i(s, a) \leftarrow Q_i(s, a) + \alpha \times [r_i + \gamma \times Q_i(s', a') - Q_i(s, a)]$
- 10 **end**
- 10 // optimal aggregation policy
- 11 $Q_{aggregate}(s, a) \leftarrow$ Aggregate($Q(s, a)$)
- 12 $s \leftarrow s'$
- 13 **end**

The MORL agent then goes after this “aggregated” single reward value and “learns” to maximize it over time.

Algorithm 1 shows the steps followed by the MORL agent in “single-policy” learning algorithm. Here, we first initialize the state s and ($N+1$) Q tables: N Q-tables corresponding to N AUs and final one is the aggregated Q table, $Q_{aggregate}$. After initialization, the various iterations, a.k.a. episodes, start for the MORL agent. The first step is to choose an action to perform. We follow an ϵ -greedy policy to choose an action based on the the current state and values

in the $Q_{aggregate}$ table. The next step is to perform the action, and after performing the action on camera (*i.e.*, changing the camera settings), the MORL agent observes the next modified state, s' , and computes the immediate reward for each AU (discussed later in Section 5.2). Following this, for each AU, the MORL agent updates the corresponding Q-table entry independently using the *bellman optimality equation*. In this equation, α is the learning rate (between 0 and 1) and γ is the discount factor (between 0 and 1). α controls the importance given to new information. The higher the value, the more importance is given to most recent information. γ controls the priority given to long-term reward or immediate reward. When γ is 1, the MORL agent values long-term rewards highly, whereas when the value is 0, the MORL agent completely ignores long-term rewards and optimizes for immediate rewards. Once the Q-table entry for each AU is computed, the MORL agent then uses an aggregation function to combine the Q-table values of each AU into an aggregate value, which is updated in the $Q_{aggregate}$ table. Finally, the state is updated to s' and the particular iteration/episode ends.

The MORL agent performs exploration and exploitation alternatively. In the ϵ -greedy policy, the value of ϵ (between 0 and 1) controls the balance between exploration and exploitation. During exploration, we run algorithm 1 for fixed K episodes to populate the Q-tables for a few hours. The MORL agent generates a random number between 0 and 1. If the random number is greater than the set value of ϵ , a random action is chosen; otherwise the “best” action for the state, *i.e.*, the one with the highest Q-value in the $Q_{aggregate}$ table is chosen. As we can see, a lower value of ϵ will trigger more random actions to be generated while a higher value of ϵ will trigger fewer random actions. The MORL agent uses a smaller ϵ (*i.e.*, 0.1) during exploration and a larger ϵ (*i.e.*, 0.9) during exploitation. Also, during exploration, the learning rate, α is set to be high (*i.e.*, 0.8), and during exploitation, it is set low (*i.e.*, 0.2) in order to assimilate new information during exploration and then use it during exploitation.

For the aggregation function used by the MORL agent, we considered three different aggregation strategies as discussed below:

- (1) **Strategy 1 (linear):** This strategy gives equal weightage to all AUs. The aggregate function, as shown in Equation 1, is computed by taking the average of the reward functions

(Q-values) obtained from the different AUs.

$$Q_{aggregate} = \sum_{i \in AU} Q_i[s, a] / count_{AU} \quad (1)$$

- (2) **Strategy 2 (weighted)**: This strategy gives different weights to different AUs according to the priorities of the AUs and computes the aggregate value by using the below Equation 2.

$$Q_{aggregate} = \sum_{i \in AU} (p_i * Q_i[s, a]) / \sum_i p_i \quad (2)$$

Such weights will be given by domain experts who understand the meaning and relative importance of the reward values for different AUs.

- (3) **Strategy 3 (winner-takes-all)**: The maximum reward (obtained using the Bellman equation) among the different rewards from multiple AUs, is used in this aggregation strategy, i.e., the winner takes all, as shown in Equation 3. Such a strategy ensures that the selected action is guaranteed to be optimal for at least one objective/AU.

$$Q_{aggregate} = \max_{i \in AU} Q_i[s, a] \quad (3)$$

5.2 AU-specific quality estimators

The MORL agent in Elixir receives individual reward functions corresponding to the multiple AUs that are running off of a single video stream, as discussed in Section 5.1. The reward function for each AU signifies whether the action taken by the MORL agent is improving or degrading the performance of the specific AU. A positive reward indicates improvement, whereas a negative reward (penalty) indicates degradation. During online operation, measuring the accuracy of the AU is not possible because accuracy measurement requires knowledge of the ground truth and such ground truth cannot be obtained in real-time. As a proxy to this accuracy measurement, the concept of AU-specific quality estimator was introduced in [24], which *estimates* the accuracy of the AU. We draw inspiration from this technique and use a similar approach in Elixir, where we develop and use new AU-specific quality estimators for the different AUs.

Specifically, the AU-specific quality estimator in Elixir consists of (1) feature extractor and (2) AU-specific quality classifier. For the feature extractor, we use the Inception-v3 [27] network up to the first inception module in order to accommodate the diverse impact of local textures. These extracted features are used by the AU-specific quality classifier to *estimate* the accuracy of the AU. We use 2-fully connected layers with 101 output classes (each output label corresponds to mAP score between 0 to 100) for the classifier.

The four AUs that we use to demonstrate the effectiveness of Elixir work are: face detection (FD), person detection (PD), car detection (CD) and license plate detection (LPD). For each of these AUs, we need to develop a corresponding AU-specific quality estimator. Although both PD and CD fall in the category of “object detection”, unlike [24], we developed new AU-specific quality estimator for each of the “object” classes, as there could be inter-class variability. Specifically, we developed separate AU-specific quality estimator for PD and CD. In addition, we developed new AU-specific quality estimators for FD and LPD.

For the development of these new AU-specific quality estimators, we used different public datasets. We picked 8000 frames from videos in Roadway [2] and LSTN [6] datasets and created ~ 4 million variants of them by applying digital transformation on these frames². These 4 million frames constitute the training dataset for FD and PD. For CD, through digital transformation on 6000 video frames extracted from Jackson and Roadway datasets [2], we created a training dataset of ~ 3 million frames. For LPD, we used 700 images from Cars [17] and AOLP datasets [9] and created 0.6 million variants using digital transformation as the training dataset.

As in [24], we use a cross-entropy loss function to train the AU-specific quality estimators, initial learning rate is 10^{-5} , and we use Adam Optimizer [16].

6 EVALUATION

We present our experimental results in this section. First, we present the results of the various AU-specific quality estimators that we developed. Then, we present the results for the different aggregation strategies considered in MORL. Next, we present the results for real-world deployment with three cameras placed next to each other running Elixir and two alternative approaches. Finally, we present some system performance results for Elixir.

6.1 AU-specific quality estimator

For MORL to work well for multiple AUs running off of a single video stream, it is very important for the rewards received for each of the AUs to be highly accurate. These rewards for individual AUs are the *estimates* given by AU-specific quality estimator for each AU. The higher the value of the *estimate*, the better the chances that the AU will give high accuracy on the frame. For evaluation of the AU-specific quality estimator, we measure the Pearson and Spearman correlation between the value of the *estimate* and the actual AU accuracy on the frame.

To evaluate AU-specific quality estimators for PD and FD, we use 2000 video frames from the video snippets extracted from Roadway [2] and LSTN [6] datasets and create 1 million variants by digitally transforming the original frames using the python-pil library [3]. These 1 million digitally transformed video frames constitute the validation dataset for PD- and FD-specific quality estimator’s performance evaluation. To evaluate CD-specific quality estimator, we create a validation dataset of 0.8 million digitally transformed images from the original 1.5K video frames extracted from the Jackson and roadway datasets [2]. For LPD-specific quality estimator evaluation, we create validation dataset of 0.2 million digitally transformed images from 500 original images extracted from the Cars [17] and AOLP datasets [9]. Note that these validation datasets are completely different from the training dataset used in Section 5.2. Once the validation dataset is created, we manually annotate the images using cvat-tool [22] and measure the AU accuracy (mAP) on these frames using the annotation as the ground truth³. Next, we obtain the *estimates* provided by the AU-specific quality estimators on these images and then measure the Pearson

²We use the python-pil library [3] for digital transformation

³We ensure that the ground-truth annotations are kept intact in the digitally transformed image variants as well.

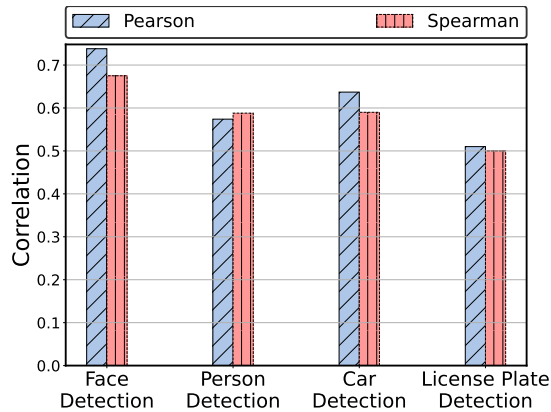


Figure 7: AU-specific quality estimator performance.

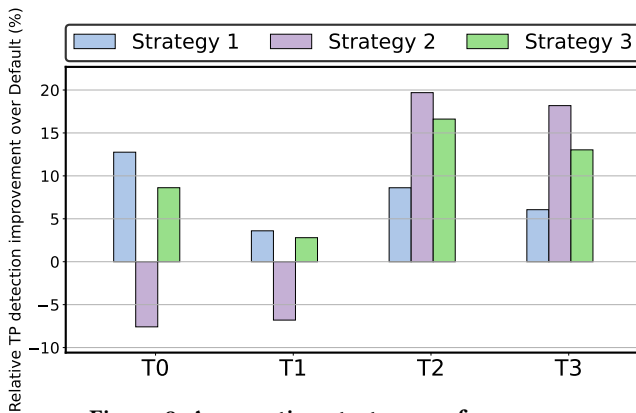


Figure 8: Aggregation strategy performance.

and Spearman correlation between the *actual* accuracy and the *estimated* value provided by the AU-specific quality estimators.

Figure 7 shows a strong positive correlation between the actual accuracy (mAP) and the provided quality estimate for the four AUs (both Pearson and Spearman correlation are greater than 0.5) [28]. This shows that *the newly developed AU-specific quality estimators provide reliable quality estimates that can be used by the MORL agent to effectively tune camera settings in order to improve accuracy for multiple AUs simultaneously.*

6.2 Aggregation strategy

Various aggregation strategies considered by the MORL agent in Elixir is described in Section 5.1. In this section, we compare these different strategies and present our experimental results.

For comparing the three strategies, we use the original video captured with default camera settings, in which two participants follow a sequence of steps as described in Section 3.1. We then annotate this video and obtain the ground-truth on the original video. Next, we create four variants of this video corresponding to different times in the day (separated by at least 2 hours each) by using the technique described in [24], which applies digital transformation on the original video to generate a variant of the original video for a different time of the day, and then label these videos as T0, T1, T2 and T3. These videos have 1000 frames each. Once we have these four videos, we project them on a monitor screen in front of a real



Figure 9: Real-world deployment setup.

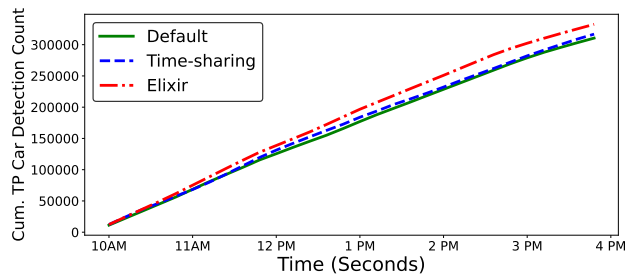
camera, as in [24], and run four different AUs, i.e., PD, FD, CD and LPD. We then compare the performance when we use the three aggregation strategies, as described in Section 5.1. For Strategy 2 (weighted), we used predefined weights of 3, 2, 1 and 1 for FD, LPD, PD and CD, respectively, based on each AU's granularity, i.e., finer the granularity of detection, more is the weight. Figure 8 shows the performance of the three aggregation strategies. We see that *Strategy 3 (winner-takes-all) performs the best when compared to the other two strategies, i.e., Strategy 1 (linear) and Strategy 2 (weighted).*

6.3 Real-world deployment

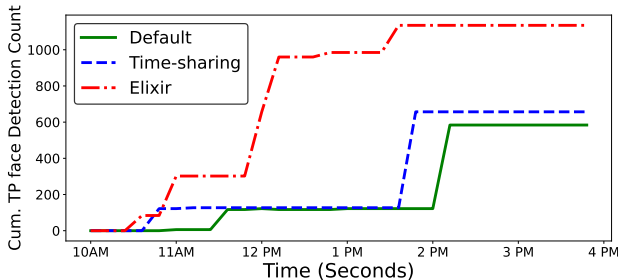
To evaluate performance of Elixir in a real-world deployment, we place three cameras next to each other as shown in Figure 9. All of them are identical cameras, i.e., AXIS Q3515 Network cameras and they overlook a large enterprise parking lot, where people park their cars and enter/exit the building. With this deployment, we are able to run multiple AUs, i.e., PD, FD, CD and LPD simultaneously on the video feed coming from a single camera. The purpose of having three cameras is to compare Elixir with other two alternative approaches. The different approaches being used on these three cameras is listed below:

- (1) **Camera 1 (Default):** Camera settings is always set to default camera settings and is never changed. All four AUs run simultaneously on the video feed from this camera with default camera settings.
- (2) **Camera 2 (Time-sharing):** Time-sharing technique is used on this camera, where each AU gets a fixed time-slot of 10 minutes and within this time-slot, camera settings are dynamically changed in favor of the specific AU for which the time-slot is allocated. Here, we deploy CamTuner [24] for each AU within its time-slot and time-slots are allocated in round-robin manner to each AU. Note that all four AUs are running simultaneously all the time, only the camera settings are changed periodically, favoring the AU for which the time-slot is allocated.
- (3) **Camera 3 (Elixir):** We deploy Elixir, which dynamically tunes camera settings to common-optimal setting that enhances data quality such that accuracy of all four AUs, i.e., PD, FD, CD and LPD is improved simultaneously

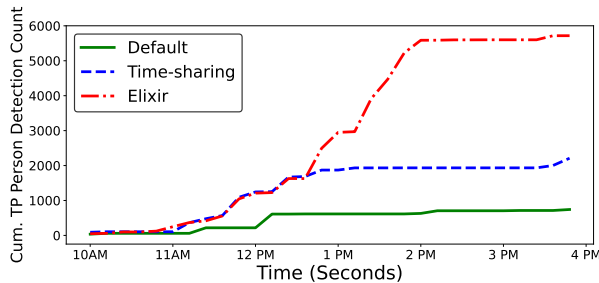
Each of these cameras upload the captured frames over 5G network to a remote edge-server (with 3.70 GHz Xeon(R) W-2145 CPU and an NVIDIA GeForce RTX 2080Ti GPU), where the four AUs



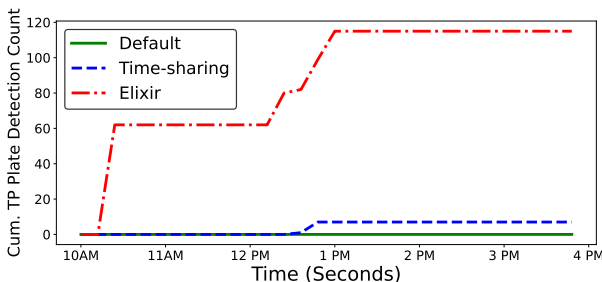
(a) Car Detection



(b) Face Detection



(c) Person Detection



(d) License Plate Detection

Figure 10: Elixir’s performance comparison with alternative approaches when four AUs are running simultaneously. We use Yolov5 [13] object detection model for PD and CD⁴, Neofacev4 [20] face detection model for FD and openalpr [21] license plate detection model for LPD. For Time-sharing and Elixir approaches, the captured frames are also sent to a low-end Intel-NUC box (with 2.6 GHz Intel i7-6770HQ CPU) where the four AU-specific quality estimators run and provide quality estimates on each frame for the four AUs, i.e., PD, FD, CD and LPD.

⁴Due to inter-class variability within same detector, we evaluate performance of person and car detection separately.

Table 5: Improvement over Elixir

Setting	PD accuracy mAP _{PD} (%) (DAY)	FD accuracy mAP _{FD} (%) (NIGHT)
<i>Common-optimal (Elixir)</i>	91.7	48.8
<i>Common-optimal (Elixir) + AU-specific digital transformation</i>	98.8	50.0

We initially perform online exploration for few hours and then start exploitation to dynamically adjust camera settings. We adjust camera settings every 30 seconds. During exploitation, we run the four AUs (on each camera) for 6 continuous hours in a day and record the videos from each camera for manual inspection. Figure 10 shows the cumulative number of true-positive car, face, person and license plate detections over the entire 6 hours for the three approaches⁵. Figure 10a shows that Elixir is able to detect 7.1% (22,068) and 5.0% (15,731) more cars than default and time-sharing approaches, respectively. Figure 10b shows that 94% (551) and 72% (478) more faces are correctly being detected by Elixir over the default and time-sharing approaches, respectively. Elixir also detects 670.4% (4975) and 158.6% (3507) more persons than the default and time-sharing approaches, respectively, as shown in Figure 10c. For license plate detection, we see that with default setting approach, none of the license plates were detected, with time-sharing approach, only 7 license plates were detected, while, with Elixir, we are able to detect 115 license plates, as shown in Figure 10d. Thus, Elixir is effective in dynamically adjusting camera settings to enhance quality of data such that accuracy of multiple AUs is improved simultaneously.

6.4 System Performance

When Elixir is deployed in operation, there are three key additional tasks that occur, when compared to normal operation with default camera settings. These three tasks are: (1) changing the camera settings, (2) computing AU-specific quality estimation for all the AUs, and (3) evaluating aggregation function to combine Q-values from all the AUs. For (1), we use Axis’ VAPIX library [4] to programmatically change camera setting. This change in camera setting takes ~ 200 ms. Since different AU-specific quality estimators use the same backbone and they run in parallel. For (2), it takes only about 48 ms to compute all AU-specific quality estimates while the CPU utilization is only around 45%. Finally, for (3), the MORL agent takes only about 1 ms to evaluate the aggregate function and update the combined value. Since Elixir runs in parallel with the AUs, it does not incur any additional delay. With respect to the delay over 5G network to upload the video frame, we observe that the latency to upload a frame is only about 39.7 ms.

7 FURTHER IMPROVEMENT OVER ELIXIR

In Table 4b, we saw that FD achieves 48.8% accuracy using the common-optimal setting, while the highest achieved accuracy using FD-optimal setting is 50%. Also, for PD, Table 4a shows that

⁵Upon manual inspection of the videos, we confirmed that Elixir does not have any false positive detections for car, face, person or license plates.

the accuracy achieved using the common-optimal setting is 91.7% while the highest achieved accuracy using the PD-optimal setting is 99.36%. Thus, there is a gap in the highest possible accuracy and the one achieved by the common-optimal setting. In this section, we show that it is possible to reduce this gap, i.e., boost the accuracy further, by applying AU-specific digital transformation on the camera feed for each AU, after Elixir tunes the camera settings to the common-optimal setting. Note that the accuracy for PD during NIGHT and the accuracy for FD during DAY, as shown in Table 4, achieve the highest possible accuracy (83.3% and 100%, respectively) already in using the common-optimal setting. Hence, we do not highlight them here.

For this study, on the frame captured with the “common-optimal” setting discussed in Section 3.1.2, we exhaustively apply different digital transformations by using the PIL library [3] and run these frames through PD and FD AUs. We then choose the digital transformation that provides the highest accuracy. Table 5 shows that the accuracy for PD is further boosted from 91.7% to 98.8% and the accuracy for FD is further boosted from 48.8% to 50%. Thus, it is indeed possible to further improve the accuracy of the AUs by applying AU-specific digital transformations on the frame, after Elixir tunes the camera settings to the common-optimal setting which works well for multiple AUs. Note that in [24], it is shown that directly applying digital transformation on frames does not improve accuracy, if the frame capture itself is of “poor” quality. Therefore, we did not directly apply digital transformations on the frames captured with default camera settings. Instead, we first let Elixir tune the camera settings to the common-optimal setting in order to enhance data quality, and then apply digital transformation on them. This “common-optimal + AU-specific digital transformation” approach gives further improvement in accuracy over Elixir.

8 CONCLUSION

When multiple video analytics tasks run on a single video stream, the optimal camera settings for each one of them is different, and the optimal camera setting for one, degrades accuracy of the other. Identifying the optimal camera setting that works well for multiple AUs and automatically adjusting it based on the changes in the environmental conditions and the video content is a very challenging task. In this paper, we present Elixir, which leverages Multi-Objective Reinforcement Learning (MORL) to dynamically adjust the camera settings such that multiple objectives (corresponding to different AUs in operation) are considered simultaneously by the RL agent to decide on the optimal camera settings that improves accuracy of multiple AUs at the same time. Through real-world experiments with four AUs running off of a single video stream, we show that Elixir correctly detects 7.1% (22,068) and 5.0% (15,731) more cars, 94% (551) and 72% (478) more faces, and 670.4% (4975) and 158.6% (3507) more persons than the default-setting and time-sharing approaches, respectively. It also detects 115 license plates, far more than the time-sharing approach (7) and the default setting (0).

REFERENCES

- [1] Allied Analytics. 2022. Global Smart Sensor Market to Reach \$91.37 Billion by 2027. <https://www.digitaljournal.com/pr/global-smart-sensor-market-to-reach-91-37-billion-by-2027>
- [2] Christopher Canel, Thomas Kim, Giulio Zhou, Conglong Li, Hyeontaek Lim, David G Andersen, Michael Kaminsky, and Subramanya Dullloor. 2019. Scaling video analytics on constrained edge nodes. *Proceedings of Machine Learning and Systems* 1 (2019), 406–417.
- [3] Alex Clark and Contributors. [n.d.]. Pillow Library. <https://pillow.readthedocs.io/en/stable/>.
- [4] Axis Communications. [n.d.]. VAPIX Library. <https://www.axis.com/vapix-library/>
- [5] Tuan Dao, Amit Roy-Chowdhury, Nasser Nasrabadi, Srikanth V Krishnamurthy, Prasant Mohapatra, and Lance M Kaplan. 2017. Accurate and timely situation awareness retrieval from a bandwidth constrained camera network. In *2017 IEEE 14th International Conference on Mobile Ad Hoc and Sensor Systems (MASS)*. IEEE, 416–425.
- [6] Yanyan Fang, Biyun Zhan, Wandu Cai, Shenghua Gao, and Bo Hu. 2019. Locality-constrained spatial transformer network for video crowd counting. In *2019 IEEE international conference on multimedia and expo (ICME)*. IEEE, 814–819.
- [7] Conor F. Hayes, Roxana Rădulescu, Eugenio Bargiacchi, Johan Källström, Matthew Macfarlane, Mathieu Reymond, Timothy Verstraeten, Luisa M. Zintgraf, Richard Dazeley, Fredrik Heintz, Enda Howley, Athirai A. Irissappane, Patrick Mannion, Ann Nowé, Gabriel Ramos, Marcello Restelli, Peter Vamplew, and Diederik M. Roijers. 2022. A practical guide to multi-objective reinforcement learning and planning. *Autonomous Agents and Multi-Agent Systems* 36, 1 (2022), 26. <https://doi.org/10.1007/s10458-022-09552-y>
- [8] Kevin Hsieh, Ganesh Ananthanarayanan, Peter Bodik, Shivaram Venkataraman, Paramvir Bahl, Matthai Philipose, Phillip B. Gibbons, and Onur Mutlu. 2018. Focus: Querying Large Video Datasets with Low Latency and Low Cost. In *13th USENIX Symposium on Operating Systems Design and Implementation (OSDI 18)*. USENIX Association, Carlsbad, CA, 269–286. <https://www.usenix.org/conference/osdi18/presentation/hsieh>
- [9] Gee-Sern Hsu, Jiun-Chang Chen, and Yu-Zu Chung. 2012. Application-oriented license plate recognition. *IEEE transactions on vehicular technology* 62, 2 (2012), 552–561.
- [10] Shubham Jain, Viet Nguyen, Marco Gruteser, and Paramvir Bahl. 2017. Panoptes: Servicing multiple applications simultaneously using steerable cameras. In *Proceedings of the 16th ACM/IEEE International Conference on Information Processing in Sensor Networks*. 119–130.
- [11] Si Young Jang, Yoonhyung Lee, Byoungheon Shin, and Dongman Lee. 2018. Application-aware IoT camera virtualization for video analytics edge computing. In *2018 IEEE/ACM Symposium on Edge Computing (SEC)*. IEEE, 132–144.
- [12] Junchen Jiang, Ganesh Ananthanarayanan, Peter Bodik, Siddhartha Sen, and Ion Stoica. 2018. Chameleon: scalable adaptation of video analytics. In *Proceedings of the 2018 Conference of the ACM Special Interest Group on Data Communication*. 253–266.
- [13] Glenn Jocher, Ayush Chaurasia, Alex Stoken, Jirka Borovec, NanoCode012, Yonghye Kwon, TaoXie, Jiacong Fang, imyhxy, Kalen Michael, Lorna, Abhiram V, Diego Montes, Jebastin Nadar, Laughing, tkianai, yxNONG, Piotr Skalski, Zhiqiang Wang, Adam Hogan, Cristi Fati, Lorenzo Mammana, AlexWang1900, Deep Patel, Ding Yiwei, Felix You, Jan Hajek, Laurentiu Diaconu, and Mai Thanh Minh. 2022. *ultralytics/yolov5: v6.1 - TensorRT, TensorFlow Edge TPU and OpenVINO Export and Inference*. <https://doi.org/10.5281/zenodo.6222936>
- [14] Daniel Kang, John Emmons, Firas Abuzaid, Peter Bailis, and Matei Zaharia. 2017. NoScope: Optimizing Neural Network Queries over Video at Scale. *Proc. VLDB Endow.* 10, 11 (Aug. 2017), 1586–1597. <https://doi.org/10.14778/3137628.3137664>
- [15] Mehrdad Khani, Pouya Hamadianian, Arash Nasr-Esfahany, and Mohammad Alizadeh. 2021. Real-time video inference on edge devices via adaptive model streaming. In *Proceedings of the IEEE/CVF International Conference on Computer Vision*. 4572–4582.
- [16] Diederik P Kingma and Jimmy Ba. 2014. Adam: A method for stochastic optimization. *arXiv preprint arXiv:1412.6980* (2014).
- [17] Jonathan Krause, Michael Stark, Jia Deng, and Li Fei-Fei. 2013. 3d object representations for fine-grained categorization. In *Proceedings of the IEEE international conference on computer vision workshops*. 554–561.
- [18] Tsung-Yi Lin, Michael Maire, Serge Belongie, James Hays, Pietro Perona, Deva Ramanan, Piotr Dollár, and C Lawrence Zitnick. 2014. Microsoft coco: Common objects in context. In *European conference on computer vision*. Springer, 740–755.
- [19] Chunming Liu, Xin Xu, and Dewen Hu. 2014. Multiobjective reinforcement learning: A comprehensive overview. *IEEE Transactions on Systems, Man, and Cybernetics: Systems* 45, 3 (2014), 385–398.
- [20] NEC. 2021. NEC Face Recognition Technology Ranks First in NIST Accuracy Testing. https://www.nec.com/en/press/202108/global_20210823_01.html.
- [21] openalpr. [n.d.]. Open-source automatic license plate recognition. <https://github.com/openalpr/openalpr>
- [22] openvinotoolkit. [n.d.]. Computer Vision Annotation Tool (CVAT). <https://github.com/openvinotoolkit/cvat>.
- [23] Arthi Padmanabhan, Anand Padmanabha Iyer, Ganesh Ananthanarayanan, Yuan-chao Shu, Nikolaos Karianakis, Guoqing Harry Xu, and Ravi Netravali. [n.d.]. Towards Memory-Efficient Inference in Edge Video Analytics. ([n.d.]).
- [24] Sibendu Paul, Kunal Rao, Giuseppe Coviello, Murugan Sankaradas, Oliver Po, Y Charlie Hu, and Srimat T Chakradhar. 2021. CamTuner: Reinforcement-Learning based System for Camera Parameter Tuning to enhance Analytics.

- arXiv preprint arXiv:2107.03964* (2021).
- [25] Faisal Z Qureshi and Demetri Terzopoulos. 2009. Planning ahead for PTZ camera assignment and handoff. In *2009 Third ACM/IEEE International Conference on Distributed Smart Cameras (ICDSC)*. IEEE, 1–8.
- [26] Navin K Sharma, David E Irwin, Prashant J Shenoy, and Michael Zink. 2011. Multisense: fine-grained multiplexing for steerable camera sensor networks. In *Proceedings of the second annual ACM conference on Multimedia systems*. 23–34.
- [27] Christian Szegedy, Vincent Vanhoucke, Sergey Ioffe, Jon Shlens, and Zbigniew Wojna. 2016. Rethinking the Inception Architecture for Computer Vision. In *2016 IEEE Conference on Computer Vision and Pattern Recognition (CVPR)*. 2818–2826. <https://doi.org/10.1109/CVPR.2016.308>
- [28] thebmj. 2019. correlation-and-regression. correlation-range.
- [29] Panrong Tong, Mingqian Li, Mo Li, Jianqiang Huang, and Xiansheng Hua. 2021. Large-scale vehicle trajectory reconstruction with camera sensing network. In *Proceedings of the 27th Annual International Conference on Mobile Computing and Networking*. 188–200.
- [30] Yi Yao, Chung-Hao Chen, Andreas Koschan, and Mongi Abidi. 2010. Adaptive online camera coordination for multi-camera multi-target surveillance. *Computer Vision and Image Understanding* 114, 4 (2010), 463–474.
- [31] Ben Zhang, Xin Jin, Sylvia Ratnasamy, John Wawrzynek, and Edward A Lee. 2018. Awstream: Adaptive wide-area streaming analytics. In *Proceedings of the 2018 Conference of the ACM Special Interest Group on Data Communication*. 236–252.
- [32] Haoyu Zhang, Ganesh Ananthanarayanan, Peter Bodik, Matthai Philipose, Paramvir Bahl, and Michael J. Freedman. 2017. Live Video Analytics at Scale with Approximation and Delay-Tolerance. In *14th USENIX Symposium on Networked Systems Design and Implementation (NSDI 17)*. USENIX Association, Boston, MA, 377–392.